CO_2 DISSOLUTION PROCESS AT GAS-LIQUID INTERFACE IN TWO-PHASE MICROCHANNEL FLOW

Yuriko Senga[1], Issei Tsutsui[1], Kohji Mishima[1], Yasuhiro Kakinuma[1] and Yohei Sato[1]
[1] Department of System Design Engineering, Keio University, Yokohama, Japan

Abstract: The CO_2 dissolution process through gas-liquid interface in microchannel flow field was investigated by a simultaneous measurement of liquid velocity and pH via micro-PIV/ LIF techniques. In order to keep static gas-liquid interface for the optical measurement, a step-shaped PDMS microchannel was fabricated in order to balance the surface tension and fluid pressure. The CO_2 concentration decreased with the increase of liquid velocity. The estimated convection and diffusion molar fluxes indicated that CO_2 transport process in water is affected by convection.

Key words: Mass transfer, CO_2 , Micro-PIV, LIF

1. INTRODUCTION

The gas dissolution process is an important process on various field such as chemical industries or environment[1]. The detailed understanding of the dissolution process in flow field will enables us elaborate control of reaction. For the purpose, it is needed to evaluate convection and diffusion spatially and quantitatively in flow field. Therefore simultaneous measurement of liquid velocity and ion concentration is conducted to obtain liquid velocity and gas concentration data. The present study organized a stable gas-liquid (GL) interface in microchannel for the measurement at first. Convection and diffusion effect on gas transport process in flow field was evaluated.

2. EXPERIMENTAL SETUP

2.1 Microchannel

For the generation of GL two phase flow, the microchannel was made as shown in figure 1. Gas was imposed in the left straight channel and liquid was driven in the right deep channel. The gas and liquid parallel flow was formed at the junction area. This microchannel was designed by considering the balance between the surface tension and the fluid pressure. The surface tension is described in Young-Laplace equation[2],

$$\Delta P_s \cong \frac{2\gamma \sin(\theta - 90°)}{d} \quad (1)$$

where γ [N/m] is the surface tension, θ [deg] is the contact angle and d [m] is the width of interface. In order to stabilize interface the surface tension was enforced through minimizing d. The liquid pressure is inverse proportion to hydraulic diameter d_e as described .

$$\Delta P_f \propto 1/d_e^{\,4} \quad (2)$$

Given equations (1) and (2), different depth channel enforce surface tension while reducing liquid pressure. For fabricating the step shaped micochannel with high accuracy, the cryogenic micromachining technique was developed as the micro milling technique for soft polymer materials. PDMS changes remarkably its elastic properties by cooling down the temperature below the glass-transition point. Figure 2 illustrates the schematic of cryogenic micromachining system. The microchannel can be processed directly on PDMS substrate immersed in the liquid nitrogen using micro milling process because PDMS is hardened like a glass under ultra low temperature of -123 centigrade (so called glass transition temperature). Three dimensional shaped microchannel can be processed precisely and rapidly by utilizing cryogenic machining. The total machining time is dramatically reduced to 100 minutes while it takes several days to process the microchannel by utilizing the conventional replica molding technique.

Thin PDMS was coated which has hydrophobic surface on the glass wall. GL interface was stabilized in a microchannel by these procedures. Ion exchanged water and CO_2 were used as the liquid and gas samples in the present experiment.

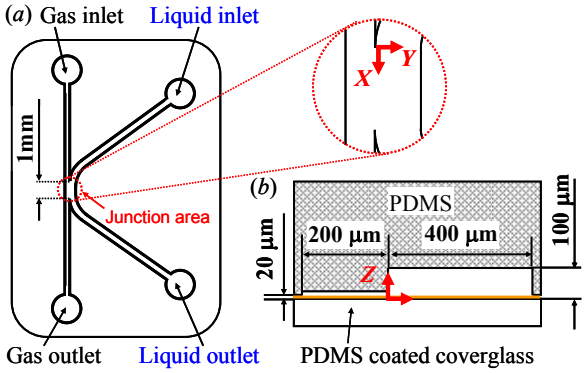

Fig. 1: (a) Top and (b) cross-sectional views of microchannel.

2.2 Measuring system

A schematic of the optical measurement system based on an inverted microscope is illustrated in figure 3. Ar laser at a wavelength of 488 nm was introduced into the confocal scanner (CSU22β Yokogawa Elec. Corp., Japan) and collected through a 20 × magnification objective lens (Nikon Corp., CFI S Fluor) with a numerical aperture (*NA*) of 0.75 into microchannel. The fluorescence from particles (Invitrogen Corp., Trans FluoSperes T8883) and dye (Wako pure chemical Inc., Sodium Fluorescein), whose properties are listed in Tables 1 and 2, passed through the objective lens and introduced into the confocal scanner. The out-of-focus fluorescence was excluded by spatial filtering at the pinhole in the confocal scanner and only in-focus fluorescence was detected by a 3CCD camera (Hamamatsu Photonics, K.K., C7780-20, 1344 ×1024 pixels, 8bits ×3). The measurement depth of 5 μm was achieved in the present experiment condition[4]. The peak values of fluorescence wavelengths from dye and particles are corresponding to the spectral response of the prism in the 3CCD camera. Therefore the sensors in the 3CCD camera could detect the different bands of fluorescence wavelength separately.

3. MEASUREMENT TECHNIQUE

3.1 Velocity measurement technique

A simultaneous measurement of liquid velocity and pH was conducted by the micro-PIV/LIF technique[5] using fluorescent particles and dye, respectively.

For the velocity measurement, particle tracking velocimetry (PTV) was utilized. In order to eliminate the effect of the Brownian motion of tracer particles, the velocity profile is obtained by spatially and temporally averaging of 99 instantaneous velocity vectors measured by PTV in the every set of measurement under the laminar flow condition with no temporal velocity variation. The measurement uncertainty in 95% confidence level of PTV with the spatial and temporal average is evaluated 10.3 μm/s. Spatial resolution is 6.2 × 24.8 μm based on the step interval of spatial average.

3.2 CO_2 concentration measurement technique

The pH distribution was obtained by Laser Induced Fluorescence (LIF) method. The fluorescent intensity, I_f [W/m^2], irradiated by the excitation intensity, I_e [W/m^2] is given by

$$I_f(\lambda, \mathrm{pH}) = I_e(\lambda) C \phi \varepsilon(\mathrm{pH}) \qquad (3)$$

where λ [nm] is the excitation wavelength, C [kg/m^2] is the concentration of fluorescent dye, ϕ [-] is the quantum efficiency and ε [m^2/kg] is the absorption coefficient which depends on pH value. A calibration

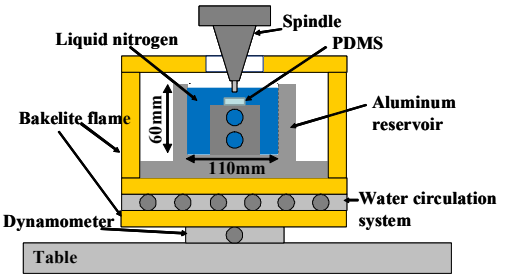

Fig. 2: The schematic of cryogenic micromachining system.

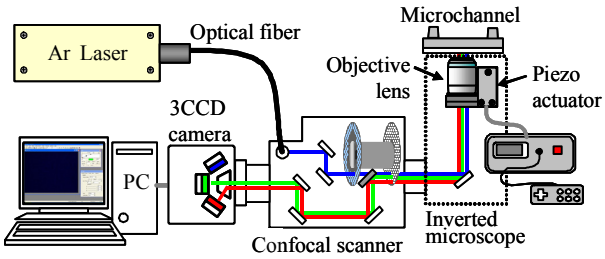

Fig. 3: Schematic of the measurement system.

Table 1: Properties of fluorescent particles.

Product name		TransFluoSpheres
Material noun		Polystyrene
Diameter	[μm]	1
Density	[g/cm^3]	1.055
Absorption wavelength	[nm]	488
Emission wavelength	[nm]	645

Table 2: Properties of fluorescent dye.

Material noun		Sodium Fluorescein
Chemical formula		$C_{20}H_{12}O_5Na_2$
Molecular weight		376.82
Absorption wavelength	[nm]	494
Emission wavelength	[nm]	518

between the fluorescent intensity and pH was conducted using five known pH aqueous solutions (pH 5.5, 6.0, 6.6, 6.9 and 7.3). In order to eliminate the influence of the nonuniform excitation light intensity normalized fluorescence intensity I_c [-] is calculated from

$$I_c = \frac{I_f(\lambda, \mathrm{pH}) - I_{\mathrm{back}}}{I_{ref}(\lambda, \mathrm{pH}_{\mathrm{ref}}) - I_{\mathrm{back}}} \qquad (4)$$

where I_{back} [W/m^2] is the background intensity detected by CCD camera, and I_{ref} [W/m^2] is the fluorescence intensity at a reference pH value. The measurement uncertainly in 95% confidence level of LIF is evaluated 0.32. The spatial resolution is 5.2 × 5.2 μm based on an average per 8 × 8 pixels.

The CO_2 concentration distribution was calculated from pH distribution by considering the CO_2 chemical equilibration in water. The CO_2 chemical equilibrium in water is described as equation (5) and (6) [6].

$$CO_2 + H_2O \rightleftharpoons H_2CO_3 \rightleftharpoons H^+ + HCO_3^- \qquad (5)$$

$$CO_2 + H_2O \rightleftharpoons H^+ + HCO_3^- \quad (6)$$

Dissolved CO_2 in water partially reacts and result in the generation of proton. Thus, dissolved CO_2 concentration can be measured from pH through these equilibrium rates. The almost all amount of dissolved CO_2 is unreacted and remains as CO_2 itself. These chemical reaction rate is represented with the use of dissolution constant K_a [mol /*l*] which is given by

$$K_a = \frac{[H^+][HCO_3^-]}{[CO_2 + H_2CO_3]} = 4.3\times10^{-7} \quad (7)$$

The relationship between pH and dissolved CO_2 concentration is derived from equation (7) as follows

$$c_{CO2} = 10^{(pK_a - 2pH)} \quad (8)$$

where $pK_a = -\log_{10}K_a = 6.35$. The CO_2 concentration in water is able to be evaluated from pH by utilizing this relationship.

4. RESULTS AND DISCUSSION

4.1 Liquid velocity and CO_2 concentration

The CO_2 dissolution process through GL interface was investigated by the present measurement system. IEW including fluorescent particles and dye was injected into right curved channel inlet. CO_2 was imposed at constant flow rate of Q_{gas}= 180 μ*l*/min in left channel. The experiment was conducted in conditions of two liquid flow rate, $U_{average}$= 1070 and 1390 μm/s respectively. Measurement area was set in the center of the junction area at x = 500 μm. The measurement was repeated at different focal positions in the vertical direction from the bottom wall (z = 0 μm) to the center of the channel (z = 50 μm) at intervals of 5 μm.

In x-y plane at z = 10 μm CO_2 dissolution process was visualized in figure 4, which presented liquid velocity and CO_2 concentration distribution. The x-y cross-sectional velocity profiles and CO_2 concentration profile were presented in figure 5 and 6. The black and white circles indicate two liquid flow rate cases. Trapezoidal velocity profile, which is the characteristic profile in the rectangular microchannel, was observed in both flow rates. The notable point is the liquid velocity in the vicinity of the GL interface appears different from opposite solid-liquid boundary where u = 0. The GL interface acts like the slip boundary. Figure 6 indicates CO_2 concentration profile. CO_2 concentration increased with the decrease of the liquid flow rate. It is supposed that the convection make a difference on CO_2 dissolution process.

The y-z cross-sectional view at x = 500 μm was shown in figure 7. It shows that CO_2 diffuse in depth-wise direction. CO_2 diffusion proceeds to the internal of the liquid phase as much as the liquid velocity decrease.

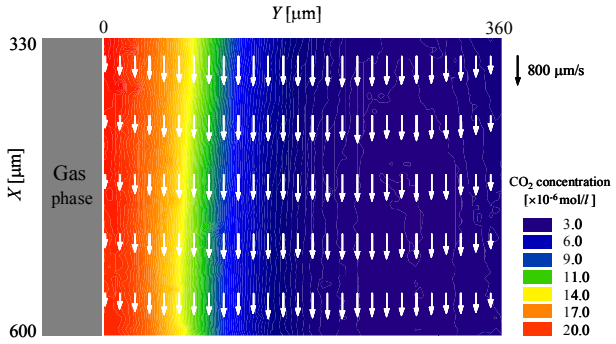

Fig. 4 : Velocity vector and CO_2 concentration contour map at z= 10 μm (U_{ave}= 1070 μm/s).

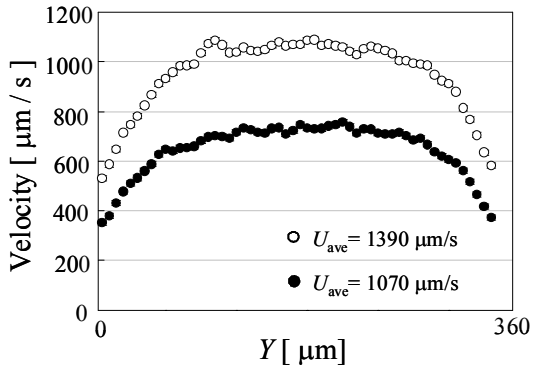

Fig.5 : Velocity profiles averaged in stream-wise direction at x = 500 μm, z = 10 μm.

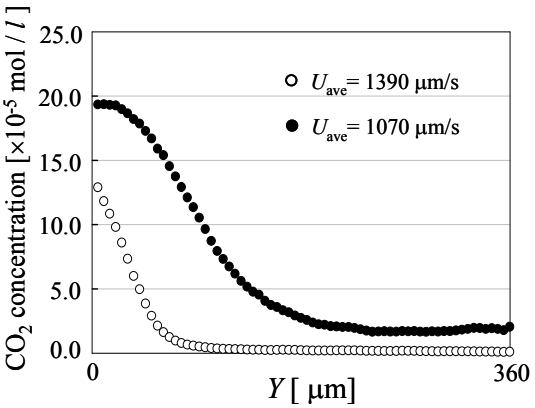

Fig. 6 : CO_2 concentration profiles at x = 500 μm, z = 10 μm.

5.2 Convection and diffusion of CO_2

For further investigation of the convection and diffusion in step-shaped microchannel, molar fluxes were calculated using experimental data. The flux of each direction consists of convection and diffusion flux, $\mathbf{J}_c$ [mol/m^{2}s] and $\mathbf{J}_d$ [mol/m^{2}s] which is expressed as

$$\mathbf{J}_c = C_{CO_2}(u, v, w) \quad (9)$$

$$\mathbf{J}_d = -D\left(\partial C_{CO_2}/\partial x, \partial C_{CO_2}/\partial y, \partial C_{CO_2}/\partial z\right) \quad (10)$$

where D [m^2/s] is the diffusion coefficient of CO_2 in water and 1.92×10^{-9} m^2/s was adopted in this experimental condition[7]. Since the y and z direction velocity component are almost zero and the CO_2 concentration gradient in stream-wise direction is negligible, the molar flux is simplified as

$$\mathbf{J} = \left(uC_{CO_2}, -D\partial C_{CO_2}/\partial y, -D\partial C_{CO_2}/\partial z\right) \quad (11)$$

The CO_2 concentration gradients were approximated in the span-wise (Y) and depth-wise (Z) direction by using central difference method from figure 6 and 7. Each component of the absolute value of molar flux at x = 500 μm was plotted in figure 8. It indicates that the x-direction flux, that is, convection flux was approximately 15 times larger than the other flux components, which means diffusion ones. From figure 8, $\mathbf{J}_x$ (U_{ave}= 1070 μm/s) has peak value at y = 58.05 μm and $\mathbf{J}_x$ (U_{ave}= 1390 μm/s) has peak value at y = 12.9 μm. The positions in which the half of the peak value were 116.1 μm and 45.1 μm respectively. From figure 6 the area where CO_2 was dissolved was estimated 98 μm and 34 μm respectively in which the half of the peak value of the CO_2 concentration. Respective value is almost the same. These facts indicate that convection is dominant in gas dissolution process so that a regulation of liquid velocity contributes to control the gas dissolution accurately.

6. CONCLUSIONS

The CO_2 dissolution into water in a microchannel was investigated by utilizing simultaneous measurement of velocity and CO_2 concentration distribution. The mass transfer process through the gas-liquid interface was observed at two liquid flow rate. The important conclusion obtained from this study is summarized below

(1) The static gas-liquid interface was realized in the microspace by controlling the channel depth and the wettability of channel wall surface. CO_2 dissolution process in flow field was investigated three-dimensionally by LIF/PTV techniques. Spatial resolution was resulted in 5.2 × 5.2 μm in LIF, and 6.2 × 24.8 × 5.0 μm in PTV respectively.
(2) CO_2 concentration and liquid velocity was captured at different focal planes. Cross sectional CO_2 concentration distribution was imaged by reconstruction of those data. CO_2 dissolved into both width-wise and depth-wise direction as much as the liquid velocity decrease.
(3) The absolute value of diffusion fluxes are approximately 15 times smaller than the convection fluxes, which means the convection is much dominant in CO_2 transfer process.

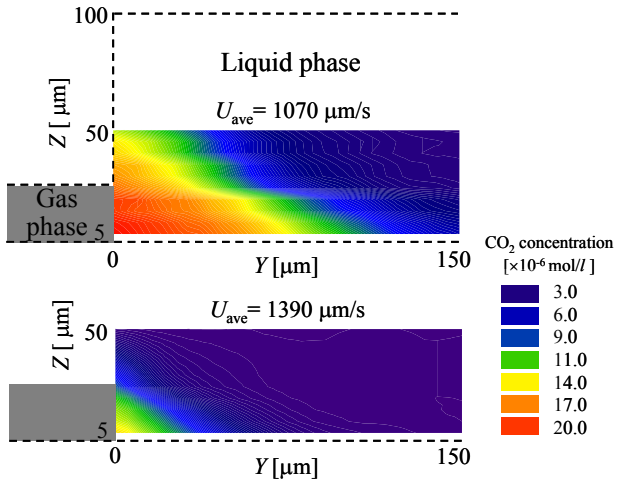

Fig. 7: CO_2 concentration contour map at x = 500 μm. (a)U_{ave} = 1390 μm/s (b)U_{ave}=1070 μm/s.

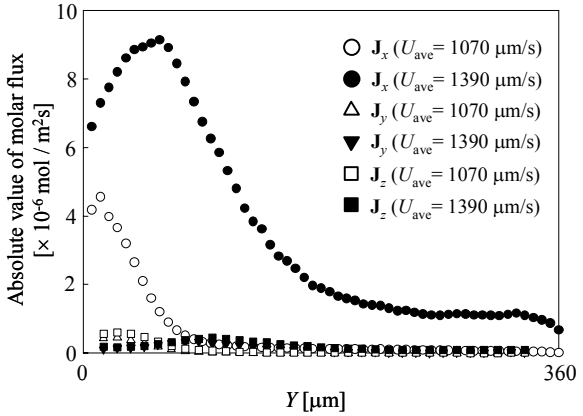

Fig.8 : The absolute value of the convection and diffusion fluxes at x = 500 μm, z = 10 μm.

ACKNOWLEDGEMENT

This work was subsidized by the Grant-in-Aid for Young Scientists (A) No.17686017 of Ministry of Education, Culture, Sports, Science and Technology.

REFERENCES

[1] Volker H, Panagiota A, Asterios G and Holger L, *Ind. Eng. Chem. Res.*, **44** (2005), 9750-9769
[2] Hibara A, Iwayama S, Matsuoka S, Ueno M, Kikutani Y, Tokeshi M, and Kitamori T, *Anal. Chem.*, **77** (2005) 943-947
[3] Kakinuma Y, Yasuda N and Aoyama T, The 4th Int. Conf. on Leading Edge Manufacturing in 21st Century of JSME, (2007), 617.
[4] Park J S, Choi C K and Kihm K D Exp. Fluids, (2004) **37,** 105-119
[5] Ichiyanagi M., Sato Y. and Hishida K., *Exp. Fluids*, **43** (2007), 425
[6] Geddes C D and Lakowicz J R, *Advanced Concepts in Fluorescence Sensing*, **9** (2005), 119
[7] Cusler E L, *Diffusion: Mass transfer in Fluid System*, Cambridge University Press (1997), 112